MOLECULAR DYNAMICS STUDY ON STRUCTURE-H HYDRATES

Robin Susilo, Saman Alavi, and John A. Ripmeester*
Steacie Institute for Molecular Sciences
National Research Council Canada
100 Sussex Drive, Ottawa, ON, K1A 0R6
CANADA

Peter Englezos
Department of Chemical & Biological Engineering
University of British Columbia
2260 East Mall, Vancouver, BC, V6T 1Z3
CANADA

ABSTRACT

The presence of structure H (sH) methane hydrate in natural environments, in addition to the well-known structure-I (sI) and II (sII) hydrates, has recently been documented. Methane in the presence of condensates (C_5-C_7) forms sH hydrate at lower pressure than the sI hydrate. Thus, the occurrence of sH methane hydrate is likely to have both beneficial and negative practical implications. On the negative side, in the presence of condensate, sH hydrate may form and plug gas transmission pipelines at lower pressures than sI hydrate. On the other hand, sH hydrate can be synthesized at lower pressures and exploited to store methane. The existence of natural hydrates containing sH hydrate may also be expected in shallow offshore areas. There are at least 26 large guest molecules known as sH hydrate formers and each of them produces a sH hydrates with different properties. The hydrate stability, the cage occupancies and the rates of hydrate formation depend on the type of large molecule selected. Consequently, it is essential to understand how the host and the guest molecules interact. Studies at the molecular-level are therefore indispensable in providing information that is not obtainable from experiments or too costly to acquire. Free energy calculations are performed to determine the relative stability among different sH hydrate systems and the preferable cage occupancy. The latter would give indications of how much methane gas can be stored in the hydrate. The interaction of guest molecule inside the hydrate cage is also investigated. The results are related to the physical and chemical properties of gas hydrates observed from the experiments or reported in the literature.

Keywords: Gas storage, clathrates, structure-H, methane, natural gas

INTRODUCTION

Gas hydrates are inclusion compounds that are formed both naturally and artificially, when water molecules and suitable guest molecule(s) are in contact at low temperatures and/or high pressure conditions [2]. The selectivity of hydrate cages toward guest molecule(s) and the gas holding potential in hydrates have attracted many scientists to investigate this compound for energy and environmental applications [3]. It is therefore important to understand thermodynamic and kinetic properties of gas hydrates. This work focuses on structure H (sH) hydrates where its occurrences in nature has been reported recently [4] and can be utilized as a promising methane storage medium [5-7]. This structure possesses the largest cage among all hydrate structures (sI, sII, and sH) and requires two different sized guest molecules to stabilize the crystal [8]. In the sH hydrate the large cages are occupied by large guest molecules whereas the smaller cages are filled with smaller molecules such as methane, xenon, or carbon dioxide, which by themselves, are known as typical sI hydrate formers. The smaller

* Corresponding author: Phone: +1 613 998 2011 Fax: +1 613 998 7833 Email: John.Ripmeester@nrc-cnrc.gc.ca

molecules (e.g. methane) may also occupy the large cage of sH hydrate with multiple occupancy, although this has been reported only at extremely high pressures and is not practical [9,10]. The large guest molecule is also known as a LMGS [11]. Interestingly, the sH hydrates with the large guest molecule (LMGS) form at lower pressures than the corresponding sI hydrates. However, the both the large and small guest molecules have low affinity with water. As a result, three separate phases: a gas phase, a non-aqueous liquid (LMGS) phase, and an aqueous phase are typically present, which complicate the system. All molecules have to be in contact for the sH hydrate to form.

Earlier experimental studies employing both macroscopic techniques (gas uptake [12,13], fluid phase equilibria [14], calorimetric [15]) and microscopic techniques (X-Ray diffraction, NMR and Raman spectroscopy [15,16]) on methane storage in sH hydrates at our laboratories revealed that the formation rates and methane occupancies differ among the three LMGS studied: *tert*-butyl methyl ether (TBME), neo-hexane (NH), and methyl-cyclohexane (MCH). The initial hydrate formation rate from solid ice powder (without stirring) [13,16] and liquid water with efficient mixing by agitation [12] were found to increase in the order: MCH<NH<TBME. The system with TBME showed the fastest initial hydrate growth rate which is consistent with the fact that TBME is much more soluble in water than NH and MCH [14] and TBME wets ice much better than the other two liquids [16]. Surprisingly, the hydrate composition determined by solid-state NMR spectroscopy and the gas content measured by decomposing the clathrate revealed that the methane content with TBME was the smallest, followed by NH and MCH [15].The methane pressure required to form a stable sH clathrate with TBME is also higher than with NH or MCH [17,18].

Moreover, the system with TBME showed a slower hydrate transformation during the formation from melted ice particles whereas the other two systems (NH and MCH) proceeded quickly towards full hydrate conversion as the temperature was ramped above the ice-point [13]. Contrary to previous findings [11,12], TBME is not the best LMGS because the total time required to convert ice/water fully into clathrate is actually longer and the methane content is also less than for the NH/MCH systems.

The experimental measurements and observations could not explain why the sH hydrate formation rate and methane content vary with LMGS. It is unknown whether different methane occupancy values observed are due to thermodynamics, kinetics or a combination of both. Hence, a molecule level study via molecular dynamics (MD) is indispensable for gaining insights on hydrate properties. Free energy calculations are performed to determine the sH hydrate stability and methane occupancy dependence on LMGS and pressure. The preference of methane molecules for different cages (5^{12} or $4^3 5^6 6^3$) is also studied. In addition, the structures of hydrate phase with LMGS is examined. The implications of these molecular level studies on hydrate stability and kinetics are discussed.

COMPUTATIONAL METHODOLOGY

The DL_POLY molecular dynamics simulation package version 2.14 was employed in this study [19]. The simulations were performed with the NPT ensemble using the Nosé-Hoover thermostat-barostat algorithm [20,21] and the modification of Melchionna et al. [22] with thermostat and barostat relaxation times of 0.5 and 2.0 ps, respectively. The equations of motion were solved by using the Verlet leapfrog algorithm with a time step of 1 fs [23,24]. The simulations were performed for a total time of 100 ps where the initial 30 ps was used to equilibrate the system.

A 3×3×3 replica of the sH hydrate unit cell with $36.99 \times 36.99 \times 29.76$ Å^3 initial dimensions and periodic boundary conditions is used as the simulation cell for the hydrate phase. The water oxygen atom positions are obtained from the crystallography of sH hydrate [25-27]. The hydrogen atoms were distributed at the oxygen sites subject to the constraints of the ice rules [28] via a Monte Carlo simulation. The sH unit cell has 34 water molecules arranged in one large 20-sided ($5^{12}6^8$) cage, two "medium" sized 12-sided cages ($4^3 5^6 6^3$), and three small 12-sided cages (5^{12}) and can be represented by $(S)_3(M)_2(L)_1 \cdot 34H_2O$, where S, M, and L represent the small, medium, and large cages, respectively. Methane molecules occupy both small and medium sH cages, whereas larger

molecule guest substance (LMGS) molecules are placed in the large hydrate cages. The LMGSs studied are *tert*-butylmethylether (TBME), neo-hexane (NH) and methyl-cyclohexane (MCH). Guest molecules are initially placed at the center of the cages and equilibrated before collecting data.

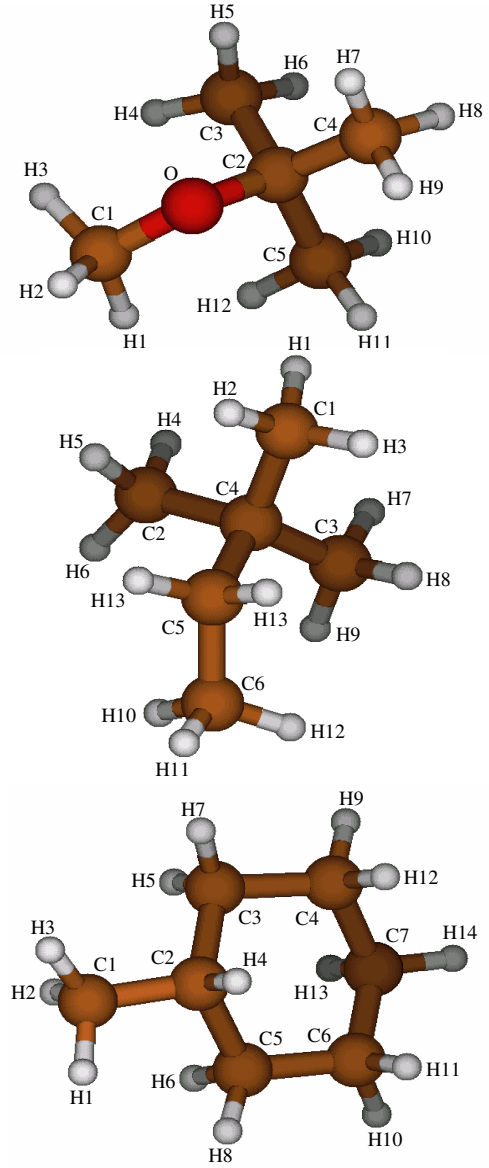

Figure 1. LMGS employed in this study: TBME (top), NH (middle) and MCH (bottom). The charges and Lennard-Jones parameters for the atoms are given in Table 1.

The van der Waals interactions among guest-guest and guest-host molecules are based on the Lennard-Jones (12-6) potential with a cut-off distance of 13 Å. Long-range electrostatic interactions were calculated using the Ewald summation method [23,24] with a precision of 1×10^{-6}. Coulombic interactions between point charges q_i and q_j located on the atomic nuclei i and j are used to model the electrostatic intermolecular interactions. The standard combination rules, $\varepsilon_{ij} = (\varepsilon_{ii}\varepsilon_{jj})^{1/2}$ and $\sigma_{ij} = (\sigma_{ii}+\sigma_{jj})/2$ are used to derive Lennard-Jones potential parameters between unlike atom-type force centers i and j from the values of the parameters between similar atom types. The intermolecular potential is given by,

$$V(inter) = \sum_{i=1}^{N-1}\sum_{j>i}^{N}\left\{ 4\varepsilon_{ij}\left[\left(\frac{\sigma_{ij}}{r_{ij}}\right)^{12} - \left(\frac{\sigma_{ij}}{r_{ij}}\right)^{6}\right] + \frac{q_i q_j}{4\pi\varepsilon_0 r_{ij}}\right\} \quad (1).$$

Atom (assignment)	Molecule	q (e)	σ_{ii} (Å) [a]	ε_{ii} (kJ/mol) [a]
O	water	−0.8476	3.166	0.6502
H	water	+0.4238	0.000	0.0000
C1 (C3)	TBME	0.1027	3.3996	0.4577
H1-H3 (H1)	TBME	0.0256	2.4714	0.0657
O (OS)	TBME	-0.5405	3.0000	0.7113
C2 (C3)	TBME	0.7721	3.3996	0.4577
C3-C5 (C3)	TBME	-0.3474	3.3996	0.4577
H4-H12 (HC)	TBME	0.0701	2.6496	0.0657
C1 (C3)	MCH	-0.3848	3.3996	0.4577
C2 (C3)	MCH	0.3597	3.3996	0.4577
C3-C4 (C3)	MCH	-0.0520	3.3996	0.4577
C5-C6 (C3)	MCH	0.0441	3.3996	0.4577
C7 (C3)	MCH	0.0265	3.3996	0.4577
H1-H3 (HC)	MCH	0.0765	2.6495	0.0657
H4 (HC)	MCH	-0.0722	2.6495	0.0657
H5-H6 (HC)	MCH	-0.0110	2.6495	0.0657
H7-H8 (HC)	MCH	-0.0050	2.6495	0.0657
H9-H10 (HC)	MCH	-0.0231	2.6495	0.0657
H11-H12 (HC)	MCH	-0.0150	2.6495	0.0657
H13-H14 (HC)	MCH	-0.0174	2.6495	0.0657
C1-C3 (C3)	NH	-0.3298	3.3996	0.4577
C4 (C3)	NH	0.6173	3.3996	0.4577
C5 (C3)	NH	0.0564	3.3996	0.4577
C6 (C3)	NH	-0.1818	3.3996	0.4577
H1-H12 (HC)	NH	0.0475	2.6495	0.0657
H13-H14 (HC)	NH	-0.0362	2.6495	0.0657
C [b]	CH_4	−0.572	3.3500	0.4257
H [b]	CH_4	+0.143	2.6100	0.0718

[a] The intermolecular potential parameters between unlike atoms are determined from combination rules.
[b] From the Murad and Gubbins potential [29].

Table 1. Atomic charges and Lennard-Jones interaction parameters used in MD simulations.

Free energy calculations were performed to determine the relative stability of sH hydrates at several methane occupancies and pressures. Initially, all small and medium cages in the simulation cell are fully occupied by methane molecules. Subsequently, in each stage methane molecules are removed or annihilated randomly from both cages to reduce the methane occupancy. The number of methane molecules annihilated from the simulation cell, x are 14, 27, 41, 54, and 68 which correspond to 0.9, 0.8, 0.7, 0.6, and 0.5 methane occupancy of the small and medium cages in the simulation cell, respectively. Two additional simulations were conducted with methane molecules removed only from the small cages or only from medium cages. This is to determine whether there is any energetic preference for the methane molecule to occupy a particular type of cage. The methane removal from the hydrate phase at temperature T and pressure p is represented by,

$$\text{hydrate } [(n+x)\ CH_4] \rightarrow \text{hydrate } [(n)\ CH_4] + x\ CH_4\ (\text{fluid}) \qquad (2),$$

where n and x are integers representing the number of methane molecules that remain in the hydrate and the number of methane molecules randomly removed from the hydrate, respectively. Chemical equilibrium is established between the two phases when methanes in the hydrate and fluid phases have the same chemical potential. The total free energy change for the methane elimination reaction in Eq. (2) is $\Delta G_{total} = G_{fluid} + (G_n - G_{n+x})$, where G_{fluid} is the free energy of methane in the fluid phase and $(G_{n+x} - G_n)$ is the free energy of n methane molecules in the hydrate phase.

For methane in the fluid phase, the free energy is the sum of ideal gas and residual contribution,

$$G_{fluid} = xkT \ln\left(\frac{\rho(T,p)}{q_{methane}}\right) + x\mu_{resid}(fluid,T,p) \qquad (3),$$

where $\rho(T, p)$ is the methane gas density, $q_{methane}$ is the partition function for methane internal degrees of freedom and $\mu_{resid}(fluid)$ is the residual (or excess) chemical potential of fluid methane at T and p. The residual chemical potential is determined from direct calculations from MD simulations by using the thermodynamic relation,

$$\mu_{resid}(fluid,T,p) = \int_1^p \left[V(p,T) - V_{ig}(p,T)\right] dp \qquad (4),$$

where $V(p,T)$ is fluid molar volume calculated from MD simulations and $V_{ig} = RT / p$ is the ideal gas molar volume at the same pressure and temperature.

The free energy of methane in the hydrate phase $(G_{n+x} - G_n)$ can be written as,

$$G_{n+x} - G_n = xkT \ln\left(\frac{\rho(hydrate,T,p)}{q_{methane}}\right) + x\mu_{resid}(hydrate,T,p) + \Delta G_{EC} \qquad (5),$$

where $\rho(hydrate,T,p)$ is the density of methane confined in the simulation cell and $\mu_{resid}(hydrate)$ is the residual chemical potential for a methane molecule from the hydrate phase. The $\mu_{resid}(hydrate)$ will be obtained by using the method of thermodynamic integration as discussed in later section. The entropy correction, ΔG_{EC} is free energy associated with the possible ways for distributing n methane molecules among a total of $n + x$ small and/or medium cages in the simulation cell,

$$\Delta G_{EC} = kT \ln\left(\frac{(n+x)!}{n!\ x!}\right) \qquad (6).$$

The total free energy change for the methane annihilation reaction in Eq. (2), is the difference between the free energies of methane in the fluid phase and methane in the hydrate phase,

$$\Delta G_{total} = xkT \ln\left(\frac{\rho(fluid,T,p)}{\rho(hydrate,T,p)}\right) + x\mu_{resid}(fluid,T,p) - x\mu_{resid}(hydrate,T,p) - \Delta G_{EC} \qquad (7).$$

The methane residual chemical potential in the hydrate phase, $\mu_{resid}(hydrate,T,p)$ is calculated by using thermodynamic integration [23] based on the Kirkwood coupling parameter method [30,31]. This technique has been used in previous free energy calculations of guest substitution and annihilation in hydrate [32-34]. The potential energy of the hydrate system can be written as [32],

$$U_{n+x}(\lambda_1,\lambda_2) = U_n + U_{elec}(\lambda_1) + U_{vdW}(\lambda_2) \quad (8),$$

where λ_1 couples the electrostatic interactions and λ_2 couples the van der Waals interactions of the x guests in the cages to the rest of the hydrate [(n)CH_4] system.

The annihilated methane molecules with $\lambda_1 = \lambda_2 = 0$ no longer interact with each other or with other remaining particles in the simulation, but remain in the hydrate simulation cell volume as ideal gas molecules at the density of the hydrate. The residual clathrate chemical potential is calculated from,

$$x\mu(hydrate,T,p) = \int_0^1 d\lambda_1 \left\langle \frac{\partial U(\lambda_1,\lambda_2)}{\partial \lambda_1} \right\rangle_{NpT,\lambda_2=1} + \int_0^1 d\lambda_2 \left\langle \frac{\partial U(\lambda_1,\lambda_2)}{\partial \lambda_2} \right\rangle_{NpT,\lambda_1=0} \quad (9).$$

The derivates of the total potential $U(\lambda_1, \lambda_2)$ with respect to the λ_i are evaluated numerically with values of λ_i between 0 and 1 in small increments [33] and these functions are used in calculating the integrals of Eq. (11).

The positions and orientations of the large guest molecule (LMGS) inside the large sH cages are examined. The atomic trajectories from MD were recorded at every 0.2 ps interval for 1000 snapshots where each snapshot consists of 27 unit cells. The analysis was done per each cage per snapshot to find unusual guest-host interactions.

RESULTS AND DISCUSSION

Preference of methane for occupying sH cages

Free energy calculations were performed to determine whether there is small or medium cage preference for methane molecule occupancy. Methane molecules from the hydrate cages were removed from the small cages, medium cages, or randomly from both small and medium cages. The different contributions to the free energies for removing 20% of the methane molecules from the clathrate are summarized in Table 2. The residual clathrate contribution to the free energy increases slightly if the methane is removed only from one particular type of cage. Moreover, there is a small entropic penalty when removing methane only from one particular cage. The total free energy calculation indicates that random methane removal from both small and medium cages is preferred over removal from only one type of cage. Hence, methane molecules are removed randomly from both small and medium cages in subsequent simulations.

θ_{CH4}	$kT\ln\frac{\rho_{fluid}}{\rho_{clath}}$	$x\mu_{resid}$ ($fluid$,T,p)	$-\Delta G_{EC}$	$-x\mu_{resid}$ (hdy,T,p)	ΔG_{total}
Small	-8.2	-0.3	-4	+19	+7
Medium	-8.2	-0.3	-3	+18	+7
Random	-8.2	-0.3	-5	+16	+3

Table 2. The contributing free energies per unit cell of removing 20% of methane molecules at 274 K and 2 MPa. All values are in kJ/mol.

Methane occupancy dependence on LMGS

The residual free energy contribution from the hydrate $-x\mu_{resid}(hydrate,T,p)$ increases linearly upon removing methane from the small and medium cages of sH hydrate for all the three LMGS at 274 K and 2 MPa as plotted in Fig. 2. The hydrate residual free energy calculations at higher pressures (6 and 10 MPa) show similar trends. The linearity shows that there are no strong collective interactions associated with the methane guests in small and medium cages. The hydrate lattice is less stable when the small and medium cages are empty.

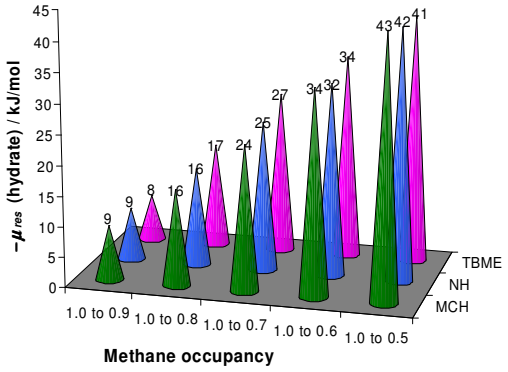

Figure 2. The residual hydrate free energy per unit cell at 2 MPa and 274 K.

Experimentally, it is observed that the methane occupancy from the sH hydrate depends on the LMGS [15]. The solid state-analysis with NMR

spectroscopy indicated that the small and medium cage occupancies increased as follows: TBME (~77%) < NH (~88%) < MCH (~90%). Similar cage occupancy values were also reported from single crystal diffraction studies [35]. If the methane occupancy dependence on LMGS were driven by thermodynamics, the hydrate residual free energy values obtained from the simulation should increase following the same trend as the measurements. However, as shown in Fig. 2, there is no noticeable difference in residual free energy among all LMGS studied within the simulation uncertainties.

This discrepancy may be related to the difference in the experimental kinetics of methane incorporation during the hydrate formation for the different LMGSs [13]. The simulations are performed under equilibrium conditions whereas the hydrates were not synthesized under constant temperature and pressure conditions. This can be an explanation for the discrepancy between the experiments and the equilibrium MD simulations. The hydrate is not formed at equilibrium although it may be expected to be at equilibrium when it is collected at the end of the experiment and the measured small/medium methane occupancies may be influenced by the formation kinetics. The change in the kinetics profile for the TBME system may be attributed to the structures of aqueous and hydrate phase in the presence of LMGS as will be discussed in later section.

Methane occupancy dependence on pressure

At given pressures and temperatures, methane molecules partition between the gas and hydrate phases. The methane molecules removed from the hydrate lattice enter the gas phase as shown in Eq. (2). The averaged residual chemical potential for the hydrate and the total free energies of the system at pressures ranging from 2 MPa to 10 MPa are plotted in Fig. 3. The residual hydrate energy is independent of pressure and LMGS but the relationship between the total free energy and methane occupancy is pressure dependent due to the fluid contributions to the total free energy, which is negative at low pressures but become more positive at higher pressures. Hence, the total free energy is fully dependent on the cage occupancy and pressure.

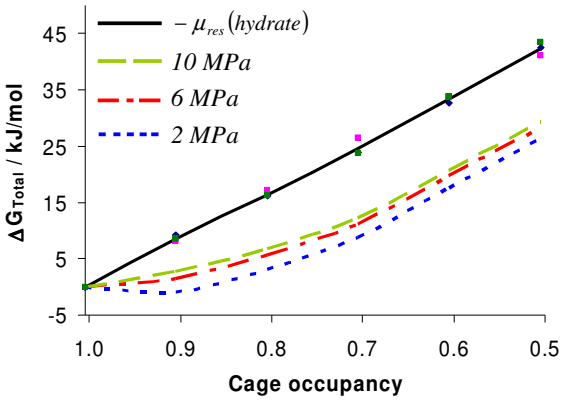

Figure 3. The residual hydrate and total free energies per unit cell at 274 K and 2-10 MPa.

At the lowest pressure (2 MPa) close to ambient pressure, the simulation predicts that the total free energy of the reaction shown in Eq. (2) is negative only when the hydrate cages go from full methane occupancy to ~90% methane occupancy. This is in good agreement with the experimental cage occupancies for NH and MCH systems [15]. Thus, less than full methane occupancies in the hydrate cages are favored near ambient conditions, as also observed in natural sI hydrate samples [36-38]. Further removal of methane molecules from the hydrate to the gas phase leads to an increase in the total free energy that eventually decreases the hydrate stability and ultimately decomposes the hydrate. At higher pressures, the total free energy of methane annihilation increases quickly, which indicates that full cage occupancies are preferred at high pressure. This observation is in good qualitative agreement with the idea of the Langmuir isotherms for gas adsorption which emphasize that higher pressure increases methane occupancy.

Hydrate cages structure with LMGS

It is well-known that water molecules form a hydration shell (cavity) when solvating a solute. The aqueous solution structure study reveals that there is a strong attraction between TBME and water molecules that lead to the formation of a hydrogen bond between oxygen-TBME and hydrogen-water [39]. Accordingly, the solvation cavity is distorted and the water molecules have a preferred orientation in comparison to the solution with hydrophobic solutes. A higher energy barrier may be required to break the hydrogen bond between TBME and water in order to form the

hydrate cage. As a result, the rate of hydrate formation with TBME is the slowest when hydrate is grown from melted ice in a non-stirred system. On the other hand, the undistorted water cavity surrounding the hydrophobic solute provides structural template required to form hydrate. Hence, the hydrate formation proceeds towards complete conversion when the temperature ramping is applied and no mass transfer resistance is present. However, it is unknown if the H-bond between the guest and host-water is present in the hydrate phase.

The guest-host interactions may also be associated with hydrate host-lattice stability, dielectric relaxation, activation energy for water dynamics and the occupancy of the cages. Guests such as ether or ketone molecules may be able to inject Bjerrum defects into the hydrate lattice by forming hydrogen bonds with cage water molecules [40]. Consequently, strong interactions between the guest and host water molecules may cause the hydrate cage to rotate faster and reduce their motional activation energy. However, there is no direct evidence on defect formation on gas hydrate, especially for sH hydrate.

Careful examinations of hydrate lattice structures obtained from MD support the hypothesis that a defect formation is possible with TBME. No defect was seen when NH or MCH was used as the LMGS. However, the host-water molecule may change its orientation towards the NH guest, although it is very rarely seen and it occurs only at high temperatures (>250 K). The large cage structure for the TBME system with and without defect is shown in Fig. 4. The cage is illustrated in two viewing side: the top and the front side at a radial distance of ~8 Å from the cage center.

The top view is on the a-b plane looking down along the c-axis. The front view is on the a-c plane looking through the b-axis. Upon looking down from the top, the large cage consists of two hexagonal rings. The ring at the center represents two hexagonal faces on the poles sides (top and bottom) and the other one on the outside represents six hexagonal faces on the equatorial plane. The outside ring looks like a perfect 12-sided from the top-view when no defect is seen. However, a distortion on the outside ring is seen as marked by the yellow dashed ellipse due to hydrogen bond that is formed between ether-TBME and host-water molecule.

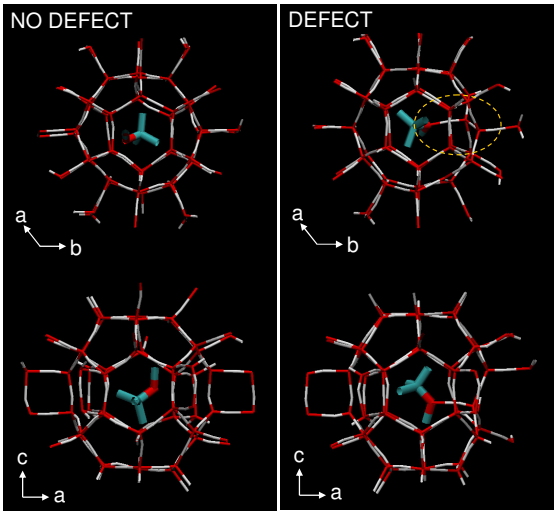

Figure 4. TBME molecule in the large cage of sH hydrate may or may not induce lattice defect.

The front view provides better illustration on the hydrate cage structure. As seen on the lower part in Fig. 4, each hexagonal faces on the equatorial plane (six in total) is connected to a medium cage which shares the square face. When no defect is formed, all square faces are seen from all the six hexagonal faces. This square face is the boundary between neighboring medium cages that are attached to the same large cage. However, this square face is altered when a defect forms. A hydrogen bond is missing on the host-cage due to the stronger attraction from the ether-TBME. Consequently, two medium cages appear as one larger cage. Hence, it is expected that the hydrate cage is less stable and less effective in enclosing the methane molecules. This is evident from the hydrate phase diagram [17,18] and methane content/cage occupancy measurements [15].

CONCLUSIONS

Molecular dynamics simulations are employed to understand the molecular-level properties of sH methane hydrate with the large guest molecules (LMGS). The methane occupancy dependence on LMGS and pressure is investigated. The structure of hydrate cage is also examined. Energetically, the hydrate lattice becomes more stable when all the cages are fully occupied. However, the negative free energy contribution from methane in the gas phase at low pressures near equilibrium conditions limits the methane occupancy in the hydrate cages and not all of the cages are fully

occupied by methane. This is in good agreement with methane occupancies of nature and synthetic hydrate samples. Full methane occupancy is favored at higher pressures. Contrary to experiments, methane occupancy dependence with LMGS was not observed in this study. This may be due to kinetic effects during the synthesis that are not taken into account in the equilibrium MD simulation. Finally, a defect formation on the large cage is observed when TBME is used as the LMGS. The defect may destabilize the hydrate lattice and limit the methane occupancies.

ACKNOWLEDGEMENTS

The financial support from Natural Sciences and Engineering Research Council of Canada (NSERC) is greatly appreciated. Robin Susilo gratefully acknowledges financial support from Canada Graduate Scholarship (CGS).

REFERENCES

[1] Susilo R, Alavi S, Lang S, Ripmeester JA, Englezos P. *Molecular dynamics study of structure H clathrate hydrate containing methane and large guest molecules*. J. Chem. Phys.; accepted for publication (March, 2008).
[2] Davidson DW. *Gas hydrates*, In *Water: a comprehensive treatise*, edited by Frank F. Plenum Press, New York, 1973.
[3] Koh CA, Sloan ED. *Natural gas hydrates: Recent advances and challenges in energy and environmental applications*. AIChE J. 2007; 53: 1636-1643.
[4] Lu H, Seo YT, Lee JW, Moudrakovski I, Ripmeester JA, Chapman NR, Coffin RB, Gardner G, Pohlman J. *Complex gas hydrate from the Cascadia margin*. Nature. 2007; 445: 303-306.
[5] Englezos P, Lee JD. *Gas hydrates: a cleaner source of energy and opportunity for innovative technologies*. Kor. J. Chem. Eng. 2005; 22: 671-681.
[6] Gudmundsson JS, Parlaktuna M, Khokhar AA. *Storing natural gas as frozen-hydrate*. SPE Prod. Facil. 1994; 9: 69-73.
[7] Mori YH. *Recent advances in hydrate-based technologies for natural gas storage-A Review*. J. Chem. Ind. Eng. (China) 2003; 54: Suppl. 1-17.
[8] Ripmeester JA, Tse JS, Ratcliffe CI, Powell BM. *A new clathrate hydrate structure*. Nature (London) 1987; 325: 135-136.
[9] Loveday JS, Nelmes RJ, Guthrie M, Belmote SA, Allan DR, Klug DD, Tse JS, Handa YP. M *Stable methane hydrate above 2 GPa and the source of Titan's atmospheric methane*. Nature (London). 2001; 410: 661-663.
[10] Loveday JS, Nelmes RJ, Klug DD, Tse JS, Desgreniers S. *Structural systematics in the clathrate hydrates under pressure*. Can. J. Phys. 2003; 81: 539-544.
[11] Tsuji H, Ohmura R, Mori YH. *Forming structure-H hydrates using water spraying in methane gas: effects of chemical species of large-molecule guest substances*. Ener. Fuels. 2004; 18: 418-424.
[12] Lee JD, Susilo R, Englezos P. *Kinetics of structure H gas hydrate*. Ener. Fuels 2005; 19: 1008-1015.
[13] Susilo R, Ripmeester JA, Englezos P. *Methane conversion rate into structure H hydrate crystals from ice*. AIChE J. 2007; 53: 2451-2460.
[14] Susilo R, Lee JD, Englezos P. *Liquid–liquid equilibrium data of water with neohexane, methylcyclohexane, tert-butyl methyl ether, n-heptane and vapor–liquid–liquid equilibrium with methane*. Fluid Phase Equilib. 2005; 231: 20-26.
[15] Susilo R, Ripmeester JA, Englezos P. *Characterization of gas hydrates with PXRD, DSC, NMR and Raman Spectroscopy*. Chem. Eng. Sci. 2007; 62: 3930-3939.
[16] Susilo R, Moudrakovski IL, Ripmeester JA, Englezos P. *Hydrate kinetics study in the presence of non-aqueous liquid by NMR spectroscopy and imaging*. J. Phys. Chem. B 2006; 110: 25803-25809.
[17] Hütz U, Englezos P. *Measurement of structure H hydrate phase equilibrium and the effect of electrolytes*. Fluid Phase Equilib. 1996; 117: 178-185.
[18] Ohmura R, Matsuda S, Uchida T, Ebinuma T, Narita H. J. *Phase equilibrium for structure-H hydrates at temperatures below the freezing point of water*. Chem. Eng. Data 2005; 50: 993-996.
[19] DLPOLY 2.14, edited by T. R. Forester and W. Smith, CCLRC, Daresbury Laboratory, 1995.
[20] Nosé S. *A Unified formulation of the constant temperature molecular dynamics methods*. J. Chem. Phys. 1984 ; 81 : 511-519.
[21] Hoover WG. *Canonical dynamics: Equilibrium phase-space distributions*. Phys. Rev. A 1985; 31: 1695-1697.
[22] Melchionna S, Ciccotti G, Holian BL. *Hoover NPT dynamics for systems varying in shape and size*. Mol. Phys. 1993; 78: 533-544.

[23] Frenkel D, Smit B. *Understanding molecular simulation*. Academic, San Diego, 2000.
[24] Allen MP, Tildesley DJ. *Computer simulation of liquids.* Oxford Science, Oxford, 1987.
[25] Davidson DW, Gough SR, Handa YP, Ratcliffe CI, Ripmeester JA, Tse JS. *Some structural studies of clathrate hydrates*. J. Phys. (Paris) 1987; 48: 537-542.
[26] Pratt RM, Mei DH, Guo TM, Sloan ED Jr. *Structure H clathrate unit cell coordinates and simulation of the structure H crystal interface with water*. J. Chem. Phys. 1997; 106: 4187-4195.
[27] Udachin KA, Ratcliffe CI, Enright GD, Ripmeester JA. *Structure H hydrate: Single crystal diffraction study of 2,2-dimethyl pentane.5(Xe,H2S).34H2O*. Supramol. Chem. 1997; 8: 173-176.
[28] Bernal JD, Fowler RH. *A theory of water and ionic solution, with particular reference to hydrogen and hydroxyl ions*. J. Chem. Phys. 1933; 1: 515-548.
[29] Murad S, Gubbins KE. in *Computer Modeling of Matter*, edited by P. Lykos. American Chemical Society, Washington, DC, 1978, pp. 62.
[30] Kirkwood JG. *Statistical mechanics of fluid mixtures*. J. Chem. Phys. 1935; 3: 300-313.
[31] McQuarrie DA, *Statistical Mechanics.* Harper & Row, New York, 1976.
[32] Alavi S, Ripmeester JA, Klug DD. *Molecular dynamics study of the stability of methane structure H clathrate hydrates*. J. Chem. Phys. 2007; 126: 124708.
[33] Yezdimer EM, Cummings PT, Chialvo AA. *Determination of the Gibbs free energy of gas replacement in sI clathrate hydrates by molecular simulation*. J. Phys. Chem. A 2002; 106: 7982-7987.
[34] Susilo R, Alavi S, Ripmeester JA, Englezos P. *Tuning methane content in gas hydrates via thermodynamics modeling and molecular dynamics simulation*. Fluid Phase Equilib. 2008; 263: 6-17.
[35] Udachin KA, Ratcliffe CI, Ripmeester JA. *Single Crystal Diffraction Studies of Structure I, II and H Hydrates: Structure, Cage Occupancy and Composition*. J. Supramol. Chem. 2002; 2: 405-408.
[36] Ripmeester JA, Lu H, Moudrakovski IL, Dutrisac R, Wilson LD, Wright F, Dallimore SR. *Structure and composition of gas hydrate in sediment recovered from Mallik 5L-38, Mackenzie Delta, N.W.T., Canada: X-ray diffraction, Raman and solid state NMR spectroscopies*. Geol. Surv. Can. Bull. 2005; 585: 106.
[37] Lu H, Moudrakovski IL, Riedel M, Spence G, Dutrisac R, Ripmeester JA, Wright F, Dallimore S. *Occurrence and structural characterization of gas hydrates associated with a cold vent field, offshore Vancouver Island*. J. Geophys. Res. 2005; 110: B10204.
[38] Hester KC, Dunk RM, White SN, Brewer PG, Peltzer ET, Sloan ED. *Gas hydrate measurements at Hydrate Ridge using Raman spectroscopy*. Geochim. Cosmochim. 2007; 71: 2947-2959.
[39] Susilo R, Alavi S, Lang S, Ripmeester JA, Englezos P. *Interactions between structure H hydrate formers and water molecules*. J. Phys. Chem. B; accepted for publication (April, 2008).
[40] Davidson DW, Ripmeester JA.*NMR, NQR and dielectric properties of clathrates*. in *Inclusion Compounds*, Vol. 3, Atwood JL, Davies JED, MacNicol DD. editors, Academic Press, London, 1984, pp. 69 – 128.